Direct numerical method to solve radiation trapping problems with a Doppler-broadening mechanism for partial frequency redistribution

A. K. Kazansky and N. N. Bezuglov
Physics Institute, St. Petersburg University, Ulianovskaya 1, 198904 St. Petersburg, Russia

A. F. Molisch
Institut für Nachrichtentechnik und Hochfrequenztechnik, Technische Universität Wien, Gusshausstrasse 25/389, A-1040 Wien, Austria

F. Fuso and M. Allegrini
INFM, Dipartimento di Fisica "Enrico Fermi," Università di Pisa, Via F. Buonarroti 2, I-56127 Pisa, Italy
(Received 26 December 2000; published 18 July 2001)

We present a numerical method for solving the Holstein-Biberman-Payne equation with Doppler frequency redistribution. The method is based on direct time propagation of the initial distribution of excited atoms, employing the split-propagation technique. It allows a precise study of various aspects of radiation transfer phenomena occurring in an arbitrary convex three-dimensional spatial region, driven by external conditions with arbitrary time dependencies. We present some results obtained for slab and spherically shaped geometries and compare them to results from other evaluation methods. The efficiency of the method is demonstrated by determining the intensity of radiation escaping the gas cell in afterglow experiments.

DOI: 10.1103/PhysRevA.64.022719 PACS number(s): 32.80.−t, 32.50.+d

I. INTRODUCTION

In optically thick media, photons can be absorbed and reemitted repeatedly before escaping from the medium. This process is known as radiation trapping [1,2] and plays an important role in various physical processes [1,3] and different engineering applications [2,4]. In laboratory conditions, dealing with both thermal and laser-cooled atomic systems (see, for instance, [5,6]) the radiation trapping has to be often carefully considered in the quantitative analysis of experimental findings [2,7,8].

It is well known that the dynamics of radiation trapping is governed by an integro-differential equation (Holstein-Biberman equation), which is very difficult to solve even in its simplest form [7,9]. The main difficulty arises from the divergence of the photon mean free path [7]. That is why studies of radiation trapping in medium geometries, i.e., gas cells, of the simplest one-dimensional shapes (infinite layer, infinite cylinder, sphere) led to a remarkable variety of specific and sophisticated techniques and approximating recipes for constructing the relevant solutions [2–4,10].

One major assumption in all early investigations of radiation trapping was that of complete frequency redistribution (CFR). This implies that the frequency of a reemitted photon is independent of the frequency of the photon that was previously absorbed. When the frequency redistribution is dominated by the Doppler effect, this assumption cannot be strictly valid: if the absorbed photon has a high-frequency shift (compared to the center frequency of the considered transition), then the absorbing atom should have a high velocity, and thus it is more probable that the emitted photon also has a high Doppler shift. This circumstance was already recognized by Holstein [9], but intentionally ignored by him to reduce mathematical difficulties. Later, Hummer [11] discussed the frequency redistribution mechanism and described the frequency redistribution function, i.e., the probability that a photon that is absorbed with frequency ν_1 is reemitted with frequency ν_2. In the following years, several methods have been developed for solving numerically[1] the generalized Holstein-Biberman equation, which includes the partial frequency redistribution. Holt [13] developed an iterative approach for computing the velocity distribution of the excited atoms (which is related to the frequencies of photons) as well as their density, but this approach is numerically efficient only at very low opacities. van Trigt [14] analyzed the limiting behavior of the trapping factor at very high opacities. We point out that an approach was already developed in Ref. [5] suitable for computing the radiation behavior during the first moments of an afterglow experiment, but this approach loses accuracy at later times.

Exact solutions at all opacities can also be obtained by various numerical methods. Among them, the Monte Carlo simulations (see, e.g., [15]) are quite popular, due to the simplicity of the relevant computer codes. However, the run time of Monte Carlo simulations quickly becomes prohibitive as the opacity increases. Two other numerical methods for solving radiation trapping problems with partial frequency redistribution are the piecewise-constant approximation (PCA) [16], and the propagator function method (PFM) [17]. It must be noted, however, that the numerical efforts required by these methods are also quite large.

A novel, highly accurate numerical method for solving the Holstein-Biberman radiation transfer equation in finite geometries has been put forward recently [18]. That method can be applied to the investigation of radiation trapping in the three-dimensional gas cells of arbitrary (convex) shape, but with the assumption of complete frequency redistribution

[1]Exact analytical solutions are only possible in infinite space, see, e.g., [12].

(CFR). In the current paper, we extend that technique to Doppler frequency redistribution (the DFR case). We show that this approach is not only accurate at all opacities, but that it also requires substantially smaller computational effort than previous methods.

II. THE BASIC TRAPPING EQUATION

The fundamental problem we address in this paper can be described with a basic equation, the generalized Holstein-Biberman equation [2,5], which determines the time evolution of the frequency-dependent density function of the excited atoms, $n^*(\mathbf{r},\nu,t)$, over the space coordinate $\mathbf{r}$ and the frequency ν (the frequency distribution is related to the velocity distribution of the atoms [3]):

$$\frac{\partial n^*(\mathbf{r},\nu,t)}{\partial t} = -A_{21}n^*(\mathbf{r},\nu,t) - A_{21}W(\mathbf{r},\nu;t)n^*(\mathbf{r},\nu,t) + A_{21}\int_{-\infty}^{\infty} d\nu' \int_{\Omega} d\mathbf{r}' G_{\nu\nu'}(|\mathbf{r}-\mathbf{r}'|) \times n^*(\mathbf{r}',\nu',t) + S(\mathbf{r},\nu,t). \quad (1)$$

The product $A_{21}n^*(\mathbf{r},\nu,t)dw\mathbf{r}d\nu$ gives the number of photons emitted spontaneously in the frequency interval $[\nu;\nu+d\nu]$ by the excited atoms contained in the volume $d\mathbf{r}$ per one second; A_{21}^{-1} is the natural lifetime of the excited state.[2] The quantity $W(\mathbf{r},\nu;t)$ is the dimensionless rate (i.e., the rate divided by A_{21}) of the nonradiative quenching of excited atoms by some (unspecified) processes. In what follows we assume that the quenching rate $W_\Omega(\mathbf{r},\nu;t)$ is very large outside a given cell of volume Ω. This trick makes sure that there are no excited-state atoms outside the cell even if we let the integration volume in Eq. (1) extend over the entire space [19]. The propagator $G_{\nu\nu'}(|\mathbf{r}-\mathbf{r}'|)$ describes the photon transfer from an emitting atom to an absorbing one. The term $S(\mathbf{r},\nu,t)$ provides a (nonstationary) source of excited atoms, e.g., their pumping via external excitation from a laser beam, energy-pooling collisions, or other mechanisms.

We note that Eq. (1) still uses several simplifying assumptions [2]. In particular, we do not consider the polarization and alignment phenomena discussed in [20]. These phenomena can be studied with the present approach by treating $n^*(\mathbf{r},\nu,t)$ not as a scalar quantity, but as a corresponding spherical tensor [21].

To formulate our problem, we specify the propagator $G_{\nu\nu'}(\rho)$,

$$G_{\nu\nu'}(\rho) = \overline{\kappa} R_{\nu\nu'} \frac{1}{4\pi\rho^2} \exp[-\rho\kappa(\nu')] \quad \text{with} \quad \overline{\kappa} \equiv \int_{-\infty}^{\infty} d\nu \kappa(\nu), \quad (2)$$

where $R_{\nu\nu'}$ is the frequency redistribution kernel and $\kappa(\nu)$ is the spectral absorption coefficient. For the case of pure Doppler broadening [5]

$$\kappa(\nu) = \kappa^{(D)}(\nu) \equiv \kappa_0^{(D)} \exp(-\nu^2), \quad \overline{\kappa} = \sqrt{\pi}\kappa_0^{(D)}, \quad (3)$$

$$R_{\nu\nu'} = \frac{1}{2}\mathrm{erf}(\max\{|\nu|,|\nu'|\}). \quad (4)$$

Here, $\kappa_0^{(D)}$ is the absorption coefficient at the center of the Doppler-broadened spectral line, and the dimensionless frequency ν is the offset of the frequency measured from the line center in units of the Doppler width $\Delta\nu^{(D)}$. It is worthy to note that a nontrivial evolution occurs only for those components of the function $n^*(\mathbf{r},\nu,t)$ that are even with respect to ν.

Actually, Eq. (1) describes a class of transfer processes broader than the conventional radiation trapping problems. Indeed, the class of problems we can treat within the present approach can be specified as those for which the ν dependence of the (spatially uniform) propagator $G_{\nu\nu'}(\rho)$ can be related to the Green's function of a second-order differential operator over a variable ν. A variety of relevant problems can be found, for instance, in plasma physics [7].

III. SPLIT PROPAGATION TECHNIQUE

Recently, we proposed a general computational algorithm [18] that allows us to investigate the radiation trapping dynamics in any arbitrary convex three-dimensional (3D) region driven by arbitrary nonstationary excitation and quenching processes. That approach has been developed only for the CFR case and here we describe its extension to DFR.

The numerical method follows directly the temporal evolution of the function $n^*(\mathbf{r},\nu,t)$ at the knots of a spatial and frequency mesh, starting from an initial distribution function. Such a method is efficient only if an algorithm exists that allows one to make one step in time propagation with a relatively small number of multiplication operations. Algorithms that achieve this with $\mathcal{O}(N\ln N)$ multiplications per time step (N is the total number of knots in the mesh used in calculation) are referred to as "fast," and their introduction ten years ago has produced proliferating activities in a number of branches of theoretical physics, such as theoretical chemical physics, theoretical atomic physics, solid-state physics, etc. (see, e.g., [22,23]). To our knowledge, there have been no attempts to apply this very powerful method to the investigation of radiation trapping processes before Ref. [18].

For solving Eq. (1) we use the so called split-propagation method [24,25] which is based on the following statement: Let the operator $\mathbf{H}$ be a sum $\mathbf{H}=\mathbf{A}+\mathbf{B}$ of two noncommuting operators. Then, the operator evolution of the system over time-step interval δt (assumed to be small enough), $\mathbf{U_H}(\delta t)$, can be approximated as a product of the partial evolution operators,

$$\mathbf{U_H}(\delta t) = \mathbf{U_A}\left(\frac{1}{2}\delta t\right)\mathbf{U_B}(\delta t)\mathbf{U_A}\left(\frac{1}{2}\delta t\right) + \mathcal{O}(\delta t^3), \quad (5)$$

[2] In what follows we set $A_{21}=1$, so that all decay times refer to the "natural" time scale.

$$\mathbf{U_D}(\delta t)\equiv\exp(-\delta t\mathbf{D}) \quad \text{with} \quad \mathbf{D}=\mathbf{A},\mathbf{B},\mathbf{H}. \tag{6}$$

Within the split propagation approach, we construct the time-propagator operator $\mathbf{U}(\delta t)$ for Eq. (1) in the following form:

$$\mathbf{U}(\delta t)=\exp\left[-\frac{\delta t}{2}W_\Omega\left(\mathbf{r},\nu,t+\frac{\delta t}{2}\right)\right]\mathcal{F}_p^{-1}\mathbf{V}_p(\delta t)\mathcal{F}_r \times\exp\left[-\frac{\delta t}{2}W_\Omega\left(\mathbf{r},\nu,t+\frac{\delta t}{2}\right)\right]. \tag{7}$$

The symbol $\mathcal{F}_r$ denotes the Fourier transform operator acting on functions

$$\mathcal{F}_r\{\zeta(\mathbf{r},t)\}\equiv\tilde{\zeta}(\mathbf{p},t)=\int\frac{d\mathbf{r}}{(2\pi)^{1.5}}\exp(i\mathbf{pr})\zeta(\mathbf{r},t) \tag{8}$$

over the space variables, while $\mathcal{F}_p^{-1}$ gives it inverse from the Fourier space variable $\mathbf{p}$ back to the coordinate variable $\mathbf{r}$. The elementary propagator $\mathbf{V}_r(\delta t)$ corresponds to the reduced equation

$$\frac{\partial n^*(\mathbf{r},\nu,t)}{\partial t}=-n^*(\mathbf{r},\nu,t)+\int_{-\infty}^{\infty}d\nu'\int_{\mathrm{R}^3}d\mathbf{r}'G_{\nu\nu'} \times(|\mathbf{r}-\mathbf{r}'|)n^*(\mathbf{r}',\nu',t), \tag{9}$$

describing the radiation transfer in an infinite space R^3 (without quenching processes).

Universally, Eq. (9) is an integral equation over the frequency variable. It seems that no universal and fast algorithm for constructing the evolution operator for such situations is known as yet. Fortunately, in the DFR case it may be directly shown that the following identity holds:

$$\left[-\frac{1}{2}\frac{\partial^2}{\partial\nu^2}+\frac{1+\nu^2}{2}\right]\exp\left(\frac{\nu^2}{2}\right)R_{\nu\nu'} =\frac{1}{2\sqrt{\pi}}\exp\left(-\frac{\nu^2}{2}\right)[\delta^{(1)}(\nu-\nu')+\delta^{(1)}(\nu+\nu')], \tag{10}$$

where $\delta^{(1)}$ is the Dirac delta function. Formally, the kernel $R_{\nu\nu'}$ in Eq. (4) is the Green's function of the second-order differential operator of a quantum oscillator type. Due to Eq. (10), Eq. (9) can be converted into the differential form in Fourier space:

$$\left[-\frac{1}{2}\frac{\partial^2}{\partial\nu^2}+\frac{1+\nu^2}{2}\right]\left[\frac{\partial}{\partial t}+1\right]\tilde{n}(\mathbf{p},\nu,t)=\Phi(\mathbf{p},\nu)\tilde{n}(\mathbf{p},\nu,t) \tag{11}$$

with $\Phi(\mathbf{p},\nu)$ given by the Fourier transform from the integral kernel $G_{\nu\nu'}(\rho)$ [3],

$$\Phi(\mathbf{p},\nu)=\frac{\kappa^{(D)}(\nu)}{|\mathbf{p}|}\arctan\left[\frac{|\mathbf{p}|}{\kappa^{(D)}(\nu)}\right]$$

and

$$\tilde{n}(\mathbf{p},\nu,t)=\exp\left(\frac{\nu^2}{2}\right)n^*(\mathbf{p},\nu,t).$$

In constructing the elementary propagation operator $\mathbf{V}_p(\delta t)$ in Fourier space corresponding to Eq. (11) written in the form

$$\frac{\partial}{\partial t}\hat{\mathbf{L}}_\nu\tilde{n}(\mathbf{p},\nu,t)=[\Phi(\mathbf{p},\nu)-\hat{\mathbf{L}}_\nu]\tilde{n}(\mathbf{p},\nu,t) \tag{12}$$

$$\text{with} \quad \hat{\mathbf{L}}_\nu\equiv-\frac{1}{2}\frac{\partial^2}{\partial\nu^2}+\frac{1+\nu^2}{2}, \tag{13}$$

we have used the Euler-type scheme

$$\hat{\mathbf{L}}_\nu\frac{\tilde{n}(\mathbf{p},\nu,t+\delta t)-\tilde{n}(\mathbf{p},\nu,t)}{\delta t} =[-\hat{\mathbf{L}}_\nu+\Phi(\mathbf{p},\nu)]\frac{\tilde{n}(\mathbf{p},\nu,t+\delta t)+\tilde{n}(\mathbf{p},\nu,t)}{2}. \tag{14}$$

From Eq. (14) it follows that

$$\tilde{n}(\mathbf{p},\nu,t+\delta t)\equiv\mathbf{V}_p(\delta t)\tilde{n}(\mathbf{p},\nu,t) =\left[\hat{\mathbf{L}}_\nu\left(1+\frac{\delta t}{2}\right)-\frac{\delta t}{2}\Phi(\mathbf{p},\nu)\right]^{-1} \times\left[\hat{\mathbf{L}}_\nu\left(1-\frac{\delta t}{2}\right)+\frac{\delta t}{2}\Phi(\mathbf{p},\nu)\right]\tilde{n}(\mathbf{p},\nu,t). \tag{15}$$

The operator $\hat{\mathbf{L}}_\nu$ in the above equation can be discretized with the uniform frequency mesh consisting of M knots with stepwidth $\Delta\nu$. The explicit representation for this operator on the mesh is obvious,

$$(\hat{\mathbf{L}}_\nu f)(\nu_j)=-\frac{1}{2d\nu^2}[f(\nu_{j+1})-2f(\nu_j)+f(\nu_{j-1})] +\frac{\nu_j^2+1}{2}f(\nu_j), \quad j=1,\ldots,M$$

$$\text{with} \quad \nu_j=\Delta\nu\left(j-\frac{1}{2}\right), \quad j=0,\ldots,M.$$

The boundary condition for solutions that are even over the frequency variable reads $f(\nu_0)=f(\nu_1)$. Apparently, the matrix of the operator $\hat{\mathbf{L}}_\nu$ is tridiagonal in this representation, and the inverse operator in Eq. (15) can be obtained with a well-known "fast" algorithm (see, for example, [26]).

IV. RESULTS AND DISCUSSION

In this section we present numerical results obtained with our approach and compare them to data from previous methods. In order to allow comparisons with previous results, we

TABLE I. Fundamental mode eigenvalues $\lambda_0 = g_0^{-1}$ for a slab geometry of total length $2L$. The left-hand side corresponds to the partial frequency redistribution case (PFR). The opacity τ is determined by $\kappa_0^{(D)}L$. The data presented were obtained using (i) the analytical method of geometrical quantization technique (GQT) developed in [19,27,28]; (ii) the present original direct numerical method (Num.); (iii) available literature sources (Others). The right-hand side of the table refers to the complete frequency redistribution (CFR) case.

	PFR			CFR		
Opacity	GQT [27]	Num.	Others [29]	GQT [19]	Num.	Others [15]
1.0	0.4792	0.4520	0.4690	0.4985	0.4580	0.492
2.0	0.3149	0.3090	0.316	0.3346	0.3174	0.331
3.0	0.2301	0.2283	0.228	0.2478	0.2371	0.245
5.0	0.1450	0.1449	0.147	0.1585	0.1524	0.157
10	0.07098	0.07076	0.0713	0.07846	0.07558	0.0773
30	0.02047	0.02039	0.0204	0.02287	0.02167	0.0223
50	0.01190	0.01105	0.0112	0.01270	0.01205	0.0125
70	0.007773	0.007514	0.00765	0.008622	0.008191	0.0851
100	0.005188	0.005001	0.0047	0.005730	0.005447	0.00566

have applied our method to the infinite slab and sphere, i.e., one-dimensional geometries. In implementing our approach, we assume that $W(\mathbf{r},\nu;t)$ is time independent and set $S(\mathbf{r},\nu,t)=0$. This describes the most common problems in radiation trapping, as, for instance, afterglow experiments. We stress, however, that none of those simplification is an essential limitation of our approach.

In our examples we have used a mesh consisting of 512 knots in the interval $[-2L;2L]$, where L is the length of the slab. The slab itself is located in the interval $[-L/2;L/2]$ and is limited by the quenching function, which is $W_\Omega(z)=0$ for $|z|<L/2$ and $W_\Omega(z)=(1-\exp\{-[(|z|-L/2)/\lambda]^2\})$ at $z\geqslant L/2$ with $\lambda=L/75$. The *s* state for the spherical geometry can be addressed within the same scheme by considering an initial state that is odd with respect to the spatial variable. We take 200 knots in the frequency domain $\nu\in[0,6]$. The time step δt in our calculation has been taken equal to 0.04. Propagation over one time step with the average class Pentium PC requires about 0.5 sec. We propagate the initial distribution over 1000 time steps, although quite reliable data can be obtained with only 100 propagation steps. The convergence has been checked by varying the number of mesh points and λ. The accuracy of calculations with the above-mentioned parameters has been found to be within at least six (decimal) digits. However, we point out a noticeable sensitivity of the trapping factors on the form of the quenching function $W_\Omega(z)$. That is due to the very abrupt change experienced by the distribution function beyond the boundary.

The escape factor for the fundamental mode can be obtained by examination of the time dependence of the autocorrelation function

$$G(t)=\int_{-2L}^{2L}dz\int_0^\infty d\nu n^*(z,\nu,t=0)\cdot n^*(z,\nu,t),$$

which can be fitted by a sum of exponential functions $\Sigma_j G_j\exp(-t/g_j)$. After a certain time, only the fundamental mode survives; at the final time T: $n^*(z,\nu,T)\simeq\exp(-T/g_0)\cdot\Psi^*_{j=0}(z,\nu)$. The higher modes $(j>0)$ can be obtained by propagation of an initial distribution function that is orthogonal to the previously calculated modes, for details see [18].

Tables I and II contain a comparison of effective radiative rate constants $\lambda_0=g_0^{-1}$ for the fundamental mode derived by our method and results available in the literature for plane and spherical geometries. The good agreement of our results with numerical Monte Carlo simulations is demonstrated also in Fig. 1, showing the behavior of the fundamental mode escape factor g_0 as a function of the opacity in a layer.

Further information on the application of our method can be derived by analyzing the frequency and space structures of modes $\tilde{\Psi}_j(z,\nu)=\exp(\nu^2/2)\Psi_j^*(z,\nu)$ for the basic Holstein-Biberman equation, Eq. (1), shown in Fig. 2. In particular, Fig. 2(a) displays the frequency dependence of the modes $j=0$ and $j=1$ (solid and dotted lines, respectively) plotted for five different positions z_i [indicated by straight vertical lines in Fig. 2(b)] for a layer with opacity 3 ($L/2=1.5$).[3] The spherical fundamental mode case (corresponding to radial modal index $n_r=0$) has been treated here as the case with plane modal index $j=1$ for the slab, assuming its length $L/2=R$. Figure 2(b) shows the spatial dependence of the mode, calculated at the line center. For the sake of clarity, in this figure the slab length $L/2$ has been slightly rescaled in the computation of the $j=1$ mode, and taken equal to 1.56.

Figure 2(a) demonstrates an important feature of the eigenmodes: their spatial and frequency dependencies can be factorized with quite high precision, since the ratio $\tilde{\varphi}_z(\nu)=\tilde{\Psi}_j(z,\nu)/\tilde{\Psi}_j(z,\nu=0)$ depends very weakly on the space position *z*. In the pictorial representation given in the figure, this circumstance leads to hardly distinguishable curves for the five different z_i positions considered. In other words, one can omit the *z* dependence of the profile $\tilde{\varphi}_z(\nu)$ and, hence, write the quite accurate relation

[3]Sometimes (as in the case of Fig. 2) it is convenient to set $\kappa_0^{(D)}=1$ and consider L as the slab opacity.

TABLE II. Fundamental mode eigenvalues λ_0 for the *s*-symmetry state in a spherical vapor cell of radius R. The opacity τ is determined by $\kappa_0^{(D)}R$. All notations are the same as for Table I.

	PFR			CFR		
Opacity	GQT [27]	Num.	Others	GQT [19]	Num.	Others [30]
0.2	0.9392	0.948		0.9462	0.9481	0.944
0.4	0.8904	0.897		0.8970	0.8995	0.896
0.6	0.8441	0.848		0.8517	0.8544	0.852
1.0	0.7601	0.7628		0.7712	0.7736	0.773
2.0	0.5981	0.6009		0.6148	0.6165	0.618
3.0	0.4841	0.4872		0.5033	0.5047	0.506
5.0	0.3391	0.3424		0.3590	0.3602	0.359
10	0.1799	0.1824		0.1956	0.1963	0.195
30	0.05333	0.05412		0.05951	0.05964	0.0597
50	0.02948	0.02976		0.03296	0.03304	0.0333
70	0.01940	0.02018		0.02228	0.02234	0.0226
110	0.01322	0.01329		0.01473	0.01473	0.0150
220	0.005983	0.005962		0.006618	0.006597	0.00671

$$\Psi_j^*(z,\nu)\cong \exp(-\nu^2/2)\tilde{\varphi}(\nu)\Psi_j^*(z,\nu=0)\equiv\tilde{\Psi}^*(z)\varphi(\nu), \tag{16}$$

playing an important role in the semiclassical treatment [27] of radiation transfer processes with partial frequency redistribution (PFR).

Figure 2(b) gives an idea of how rapidly the modes vanish outside the layer due to the presence of the quenching function $W_\Omega(z)$ determined above.

By analyzing the eigenmode structure, one can infer that the problem of trapped radiation escape from a cell with a certain initial space and frequency distribution of the excited atoms, $n^*(z,\nu,t=0)$, consists of two stages. At the first stage, prompt relaxation of initial frequency distribution to the lowest-frequency mode occurs in the time scale of a natural radiation lifetime [27,31]. Then, the frequency relaxation is concluded and spatial relaxation within the manifold of the eigenmodes related to the lowest-frequency mode proceeds, which is a substantially slower process. Qualitatively, this stage resembles relaxation of the excited atoms for the CFR case, since for the fundamental modes the DFR and the CFR cases are rather similar (see escape factor data in Tables I and II). When considered together, these two mechanisms can produce interesting peculiarities in the time dependence of the escaping radiation intensity $J(t)$, which can be calculated as the time derivative of the total number $N(t)\equiv\int_{-L/2}^{L/2}dz\int_{-\infty}^{\infty}d\nu n^*(z,\nu,t)$ of the excited atoms,

$$J(t)\equiv -\frac{1}{N(t=0)}\frac{d}{dt}N(t), \quad \int_0^\infty dtJ(t)=1.$$

If a photon escapes from the cell, the integrated excited-state density must decrease by one emitting atom. Note that the normalization condition on $J(t)$ corresponds to one excited atom at time $t=0$. In Fig. 3 we give an example of $J(t)$ for a few values of the frequency ν_i, which determines the center of initial spectral distribution of the atoms, taken in the form

$$n^*(z,\nu,t=0)=N^*(z,t=0)\varphi(\nu,t=0)$$

$$=\exp[-400z^2/(L^2)]\exp[-10(\nu-\nu_i)^2]. \tag{17}$$

The present approach turns out to be a perfect tool for direct investigation of various nonstationary problems and it allows one to follow directly the time evolution of the excited atom distribution in the cell.

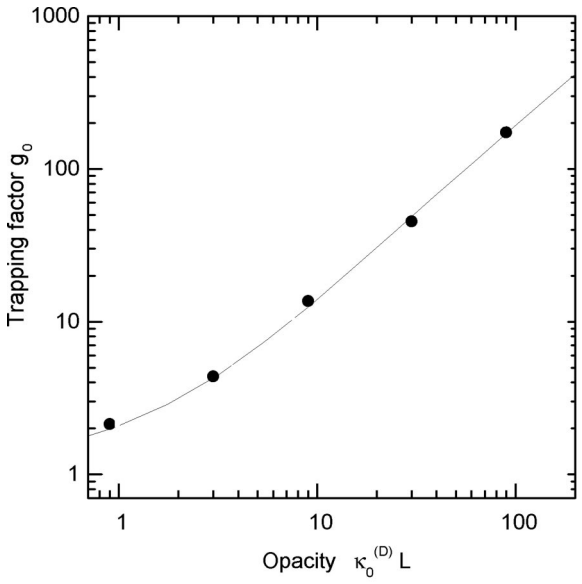

FIG. 1. Fundamental mode escape factor g_0 for a layer of total length L as a function of the dimensionless opacity $\tau=\kappa_0^{(D)}L$. The solid line corresponds to the present numerical method; dots are the results of a Monte Carlo simulation [21] for the PFR case.

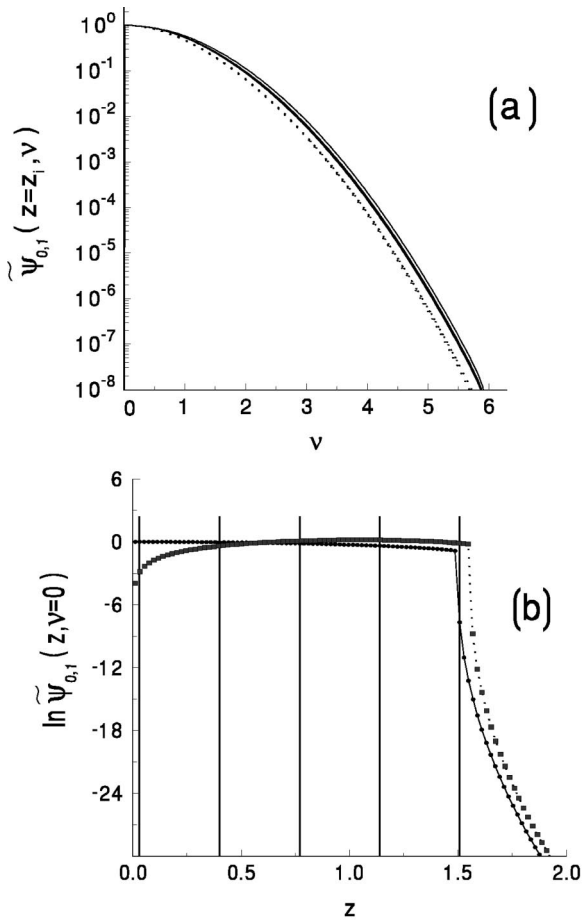

FIG. 2. Illustration of the factorization property, Eq. (16), for modes $\Psi_j^*(z,\nu)$. (a) Frequency dependence of the two first modes $\tilde{\Psi}_j(z_i,\nu)$ with $j=0,1$ (solid and dotted lines, respectively) plotted in the case of a slab with opacity $\kappa_0^{(D)}L=3$ for five different positions z_i [corresponding positions are indicated by vertical straight lines in the plot of panel (b)]. The dimensionless variable ν is the detuning measured in units of the Doppler width $\Delta\nu^{(D)}$. All curves are normalized to the unit value at the line center; note that, due to the weak dependence of the function on the space coordinate discussed in the text, curves for different positions appear hardly distinguishable from each other and no labeling can be applied. (b) Space dependence of the two first modes $\tilde{\Psi}_j(z,\nu=0)$ with $j=0,1$ (solid and dotted lines, respectively) for the same slab as in panel (a), but, for the sake of clarity, the slab opacity has been rescaled to 3.12 for the second mode ($j=1$). We assume $\kappa_0^{(D)}=1$ and, thus, consider the dimensionless coordinate z as the opacity of the gas layer situated between the space point z and the slab center.

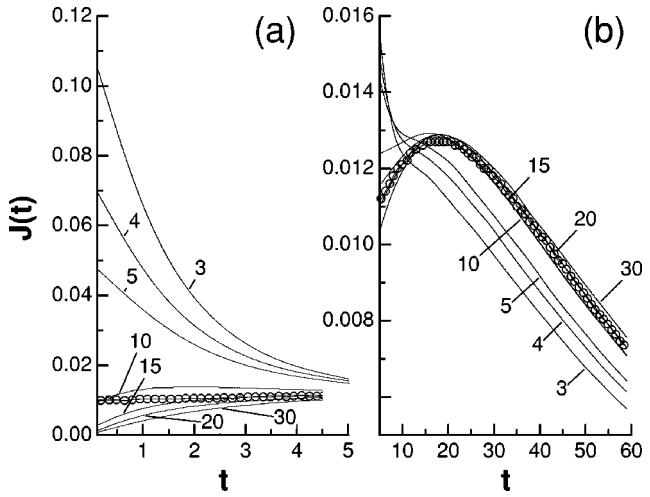

FIG. 3. Temporal behavior of the total intensity $J(t)$ of escaping radiation under afterglow conditions. Initially a slab of total length L with opacity $\tau=30$ is excited at its central part $|z|<0.1(L/2)$ in accordance with Eq. (17). The initial frequencies ν_i of the excitation are related to the opacities $\tau_i=\tau\exp(-\nu_i^2)=30$, 20, 15, 10, 5, 4, 3, as specified close to each curve. The dotted line represents the CFR case. Time t and intensity $J(t)$ are measured in units of spontaneous decay lifetime A_{21}^{-1} and radiative rate constant A_{21}, respectively. Panels (a) and (b) display initial and intermediate stages of the decaying process, respectively. Note the different horizontal and vertical axes.

In the curves presented in Fig. 3 one can discern the two stages described above. First [Fig. 3(a)], the intensities of the radiation for different initial ν_i reaches an approximately unique value, which is related to the relaxation of the frequency modes to the lowest mode with the Doppler distribution (dotted curve). This stage strongly depends on the value of the central frequency ν_i, which determines the intensities of various frequency modes in the expansion of the initial frequency distribution over the eigenmodes. At the second stage [Fig. 3(b)], relaxation of the spatial modes related to the lowest-frequency mode occurs. A specific growth of the intensity $J(t)$ at some stage of the decay process [32] can be of importance in practically occurring experimental conditions. It can take place because the coefficients in the expansion of the initial state, projected on the lowest-frequency mode, can carry different signs for different spatial modes, see also [27]. Figure 3 should be compared with Fig. 7 in Ref. [27], where the same intensities $J(t)$ have been calculated within the frame of the analytical geometrical quantization technique (GQT). One can infer that both methods give very similar quantitative results. Some deviations between our $J(t)$ curves and those in [27] are related to the different representation of the initial frequency distribution function $\varphi(\nu,t=0)$, which in the semiclassical calculations was taken as a δ function $\varphi(\nu,t=0)=\delta^{(1)}(\nu-\nu_i)$ instead of the form employed here, Eq. (17).

As a curious example, useful to better point out the capabilities of our method, we demonstrate in Fig. 4 one more possible type of decaying fluorescence $J(t)$ for an initial frequency profile $\varphi(\nu,t=0)$ with a DFR mechanism. Atoms, first excited by monochromatic laser pulses at frequency ν_i, then emit photons in accordance with Eq. (4),

$$n^*(z,\nu,t=0)=\exp[-400z^2/(L^2)]\,\mathrm{erf}(\max\{|\nu|,|\nu_i|\}). \tag{18}$$

The most interesting feature of decaying processes involving radiation trapping with DFR appears in Fig. 4 as a sequence of decreasing-increasing-decreasing slopes[4] for some of the

[4]We call attention to the fact that no cascade processes can occur in a system of two-level atoms discussed here.

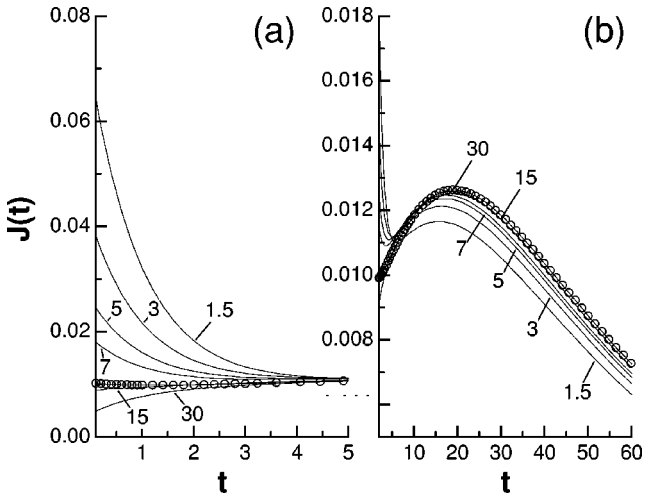

FIG. 4. Same as Fig. 3, but the initial frequency-dependent excited atoms distribution is taken as described in Eq. (18).

displayed $J(t)$ curves, namely those calculated for frequencies ν_i with $\tau_i = 7,5,3$. Obviously, tailoring of the initial profile of excited atoms can allow one to obtain various time dependencies of the escaping radiation intensity, worth to be demonstrated in specific experimental conditions.

V. CONCLUSIONS

We have presented a method for the computation of radiation trapping with partial frequency redistribution due to the Doppler effect. This method is extremely efficient numerically. It computes the time evolution of the excited-state distribution, using only $\mathcal{O}(N \ln N)$ multiplications for each time step, where $N = N_r M_\nu$, i.e., the total number of discretization points in the space-frequency mesh. It is worthwhile to compare our technique to previously proposed computation methods. In the propagator function method [17], one deals with a similar mesh, and also directly computes the temporal evolution. Since the propagation from each discretization point to each other is computed, the numerical effort is $\mathcal{O}(N^2)$. Considering the large number of discretization points one needs in PFR problems, the savings offered by our method is significant. A comparison of the numerical effort of Monte Carlo simulations is somewhat more difficult, since it strongly depends on the required accuracy. The number of photons that have to be simulated depends on the square of the required accuracy, so that they are suitable mainly for ''quick-and-dirty'' simulations. Furthermore, their implementation is more problematic at high opacities. For our method, as well as the PFM, we can increase the stepsize of the temporal evolution when observing the decay of the spatial modes. For Monte Carlo simulations, a similar approach requires sophisticated ''weighting'' of photons and is furthermore numerically unstable [2].

Comparison to the piecewise-constant approximation also demonstrates the advantage of the present method. Since it requires the solution of an eigenvalue problem, the numerical effort increases with N as $\mathcal{O}(N^3)$. On the other hand, it does not require progression through time steps, and gives all modes simultaneously. Its main drawback is, however, the large storage requirements, and also numerical problems in many commercial eigenvalue solving packages, when N becomes large.

Our method is efficient and numerically robust for a large range of parameters. We have used it to point out some fundamental properties of the decay process with DFR. Especially, the decay of the higher-frequency modes takes place on a much faster scale (essentially one natural lifetime) than the decay of the spatial modes. A very promising feature of the present approach is related to its applicability to direct and exhaustive investigation of fast nonstationary processes. This feature may be the most important advantage of the method, since spectroscopic methods requiring the separation of ultrafast signals are currently being developed.

Future investigations will concentrate on extending our approach to other types of redistribution functions. We would suggest that the approximate factorization of modes expressed by Eq. (16) is a fundamental property of the problem. Note that the factorization of the eigenmodes is equivalent to the separation of space and frequency variables and its validity can be demonstrated within the semiclassical approximation [27]. The purpose of further numerical simulations is both testing this hypothesis and treating radiation energy-transfer effects for more general experimental situations including, for instance, a system of cold atoms obtained in magneto–optical traps [6].

Another, more traditional, field of the split-propagation technique applications deals with solution of local diffusion equations of the Fokker-Planck type widely occurring in plasma physics (kinetic Boltzmann equations) and chemistry physics (diffusion equations). The above described trick, reducing the account for boundary conditions to entering quenching rate functions into kinetic equations, allows us to study different problems with nonstationary parameters of phase volumes. We mention, as an example, a stochastic walk of a Rydberg electron in an elementary collision reaction [33] where changes of the available ''size'' of the energy space for the bound optical electron are caused by an internuclear motion of colliding atoms.

ACKNOWLEDGMENTS

We are grateful to NATO for financial support via the Linkage and Networking program (under Grant No. PST.CLG 975350). We also acknowledge financial support from the Russian Foundation for Basic Research, Project No. 00-03-32926. The work has been also carried out within the framework of the Italo-Russian agreement for Scientific and Technological Cooperation 2000-2002, No. FIS2.

[1] A. G. Mitchell and M. W. Zemanski, *Resonance Radiation and Excited Atoms* (Cambridge University Press, Cambridge, 1961).
[2] A. F. Molisch and B. P. Oehry, *Radiation Trapping in Atomic Vapours* (Oxford University Press, Oxford, 1998).
[3] V. V. Ivanov, *Transfer of Radiation in Spectral Lines*, NBS Special Publ. No. 385 (U.S. GPO, Washington, D.C., 1973).
[4] N. C. van de Hulst, *Multiple Light Scattering* (*Tables, Formulae, and Application*) (Academic Press, New York, 1980), Vols. 1 and 2.
[5] M. G. Payne, J. E. Talmage, G. S. Hurst, and E. B. Wagner, Phys. Rev. **181**, 97 (1969).
[6] A. Fioretti, A. F. Molisch, J. H. Muller, P. Verkerk, and M. Allegrini, Opt. Commun. **149**, 415 (1998).
[7] L. M. Biberman, V. S. Vorobjev, and I. T. Yakubov, *Kinetics of Nonequilibrium Low-Temperature Plasma* (Plenum, New York, 1987).
[8] A. Corney, *Atomic and Laser Spectroscopy* (Oxford University Press, Oxford, 1977).
[9] T. Holstein, Phys. Rev. **72**, 1212 (1947); **83**, 1159 (1951).
[10] C. van Trigt, Phys. Rev. **181**, 97 (1969); Phys. Rev. A **1**, 1298 (1970); **4**, 1303 (1971); **13**, 726 (1976).
[11] D. G. Hummer, Mon. Not. R. Astron. Soc. **125**, 21 (1962).
[12] V. I. Perel' and I. V. Rogova, Zh. Éksp. Teor. Fiz. **65**, 1012 (1973) [Sov. Phys. JETP **38**, 501 (1974)].
[13] H. K. Holt, Phys. Rev. A **13**, 1442 (1976).
[14] C. van Trigt, Phys. Rev. A **13**, 726 (1976).
[15] A. F. Molisch, B. P. Oehry, and G. Magerl, J. Quant. Spectrosc. Radiat. Transf. **48**, 377 (1992).
[16] A. F. Molisch, B. P. Oehry, W. Schupita, and G. Magerl, Comput. Phys. Commun. **77**, 255 (1993).
[17] G. J. Parker, W. N. G. Hitchon, and J. E. Lawler, J. Phys. B **26**, 4643 (1993).
[18] A. K. Kazansky and N. N. Bezuglov, J. Phys. B **33**, 99 (2000).
[19] N. N. Bezuglov, A. F. Molisch, A. N. Klucharev, F. Fuso, and M. Allegrini, Phys. Rev. A **57**, 2612 (1998).
[20] M. I. D'yakonov and V. I. Perel', Zh. Éksp. Teor. Fiz. **47**, 1483 (1964) [Sov. Phys. JETP **20**, 997 (1965)].
[21] A. Hishikawa, T. Fujimoto, and P. Erman, Phys. Rev. A **52**, 189 (1995).
[22] *Time-dependent Quantum Molecular Dynamics*, edited by J. Broeckhove and L. Lathouwers (Plenum Press, New York, 1992).
[23] *Numerical Grid Methods and Their Application to Schrödinger's Equation*, edited by C.Cerjan (Kluwer Academic Publishers, Dordrecht, 1993).
[24] M. D. Fiet, J. A. Fleck, and A. Steiger, J. Comput. Phys. **47**, 412 (1982).
[25] M. D. Fiet and J. A. Fleck, J. Chem. Phys. **78**, 301 (1982); **80**, 3578 (1984).
[26] W. H. Press, S. A. Teulkovsky, W. T. Vetterling, and B. P. Flannery, *Numerical Recipes in Fortran. The Art of Scientific Computing*, 2nd ed. (Cambridge University Press, Cambridge, 1993).
[27] N. N. Bezuglov, A. K. Kazansky, F. Fuso, and M. Allegrini, Phys. Rev. A **63**, 042703 (2001).
[28] N. N. Bezuglov, A. F. Molisch, A. N. Klucharev, F. Fuso, and M. Allegrini, Phys. Rev. A **59**, 4340 (1999).
[29] A. F. Molisch, G. J. Parker, B. P. Oehry, W. Schupita, and G. Magerl, J. Quant. Spectrosc. Radiat. Transf. **53**, 269 (1995).
[30] A. F. Molisch, B. P. Oehry, W. Schupita, and G. Magerl, J. Quant. Spectrosc. Radiat. Transf. **49**, 361 (1993).
[31] V. V. Ivanov and V. V. Schneeveis, Astrofizika **12**, 245 (1976).
[32] P. Wiorkowski and W. Hartman, Opt. Commun. **53**, 245 (1985).
[33] N. N. Bezuglov, V. M. Borodin, A. N. Klucharev, F. Fuso, M. Allegrini, K. V. Orlovsky, and M. L. Ianson, Opt. Spectrosk. **86**, 922 (1999) [Opt. Spektrosc. **86**, 824 (1999)].